SUPERVISION EXISTS EVERYWHERE: A DATA EFFICIENT CONTRASTIVE LANGUAGE-IMAGE PRE-TRAINING PARADIGM

Anonymous authors
Paper under double-blind review

ABSTRACT

Recently, large-scale Contrastive Language-Image Pre-training (CLIP) (Radford et al., 2021) has attracted unprecedented attention for its impressive zero-shot recognition ability and excellent transferability to downstream tasks. However, CLIP is quite data-hungry and requires 400M image-text pairs for pre-training, thereby restricting its adoption. This work proposes a novel training paradigm, Data efficient CLIP (DeCLIP), to alleviate this limitation. We demonstrate that by carefully utilizing the widespread supervision among the image-text pairs, our DeCLIP can learn generic visual features more efficiently. Instead of using the single image-text contrastive supervision, we fully exploit data potential through the use of (1) self-supervision within each modality; (2) multi-view supervision across modalities; (3) nearest-neighbor supervision from other similar pairs. Benefiting from these intrinsic supervision, our DeCLIP-ResNet50 can achieve 60.4% zero-shot top1 accuracy on ImageNet, which is 0.8% above the CLIP-ResNet50 while using 7.1× fewer data. Our DeCLIP-ResNet50 outperforms its counterpart in 8 out of 11 visual datasets when transferred to downstream tasks. Moreover, Scaling up the model and computing also works well in our framework.

1 INTRODUCTION

Over the last few years, pre-trained models have greatly revolutionized computer vision (CV) and natural language processing (NLP). The first wave of exploring pre-trained models took place in the field of CV. Deep convolutional neural nets (Krizhevsky et al., 2012; Simonyan & Zisserman, 2014; He et al., 2016) are pre-trained on well-labeled ImageNet (Deng et al., 2009) and then transferred to downstream CV tasks (Girshick et al., 2014; Long et al., 2015; Vinyals et al., 2015). Standardly, CV models are pre-trained to predict a fixed set of pre-defined object categories, e.g., 1000 classes in ImageNet. However, this supervised pre-training is hard to scale since we need arduous human labeling to specify new visual concepts.

When pre-training meets NLP, the intrinsic supervision within the natural language makes the pre-training more scalable (Devlin et al., 2018; Radford et al., 2019; Brown et al., 2020). Witnessing the progress in NLP, researchers use natural language supervision to learn visual features. The language-image pre-training can scale up to a very large size, benefiting from abundant image-text pairs on the Internet. For instance, CLIP (Radford et al., 2021) and ALIGN (Jia et al., 2021) adopt the contrastive loss to push the embedding of matched image-text pairs together while pushing those of non-matched pairs apart. They achieve prestigious performance by learning from an enormous dataset that contains 400M/1B image-text pairs. However, these methods also require huge storage and computing resources, which is not affordable for most laboratories and companies. We argue that these prior arts only use the single image-text contrastive supervision while overlooking the widespread supervision within the pairs, thus is inefficient.

Firstly, there underlies rich structural information within each modality itself (LeCun & Misra, 2021). We can tweak some words/pixels in a sentence/image while retaining a similar semantic meaning. This sort of self-supervision can be exploited to learn a more common-sense representation for each modality (Devlin et al., 2018; He et al., 2020; Chen et al., 2020a). Moreover, inspired

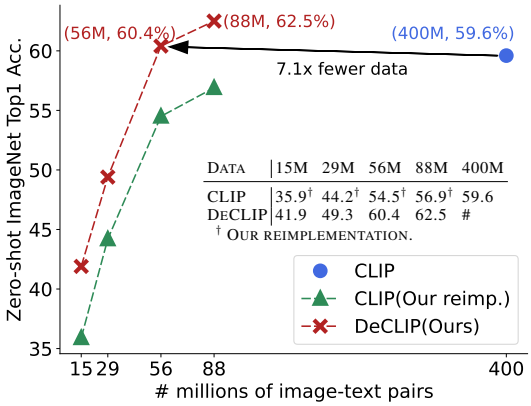

Data	15M	29M	56M	88M	400M
CLIP	35.9†	44.2†	54.5†	56.9†	59.6
DeCLIP	41.9	49.3	60.4	62.5	#

† Our reimplementation.

Figure 1: Zero-shot performance of CLIP-ResNet50 and our DeCLIP-ResNet50 when using different amounts of data. (88M, 62.5%) denotes the use of 88M data with top-1 accuracy 62.5% on the ImageNet-1K validation dataset. Our model has much better data efficiency.

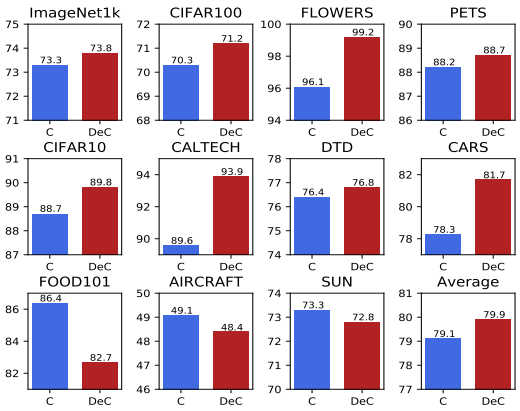

Figure 2: Transfer the DeCLIP-ResNet50 (abbr. as DeC) and CLIP-ResNet50 (abbr. as C) to 11 downstream visual datasets using linear probe verification. Our DeCLIP achieves better results in 8 out of 11 datasets.

by contrasting multi-crops in an image (Caron et al., 2020), we further extend the multi-view [1] supervision into our multi-modality setting. Specifically, each image is paired with multiple textual descriptions obtained via stochastic augmentations, vice versa. The benefit is intuitive: this auxiliary multi-view supervision brings more invariant and robust information.

Besides these overlooked supervision, we propose a novel nearest-neighbor (NN) supervision from other similar pairs. This NN supervision is mainly based on the intuition that one image is likely to have other similar text descriptions among the dataset. As shown in right figure, the image with the text `'going to see a lot of vintage tractors this week'` can also be described by `'vintage at tractors a gathering'`. For this reason, we sample the NN in the embedding space and utilize them as additional supervisory signals. Aggregating these supervision leads to our novel training paradigm DeCLIP, which stands for **D**ata **e**fficient **C**ontrastive **L**anguage-**I**mage **P**retraining.

Figure 3: Examples of Nearest Neighbor from Conceptual Captions dataset.

Extensive experiments show the effectiveness and efficiency of our DeCLIP. As shown in Fig. 1, with a ResNet50 image encoder and a Transformer text encoder, our model can achieve 60.4% zero-shot top1 accuracy on ImageNet, which is 0.8% above the CLIP-ResNet50 while using 7.1× fewer data. Using only 88M image-text pairs, our best ResNet50/ViT-B32 models boost the zero-shot performance to 62.5% and 66.2%, nearly 3.0% higher than the best number reported for these two architectures. We further verify the transferability of our models on downstream tasks. As indicated in Fig. 2, our DeCLIP-ResNet50 outperforms its counterpart in 8 out of 11 visual datasets. Moreover, Scaling up the model and computing also works well in our framework. Using 4.5× fewer data, our DeCLIP-RegNetY-64GF achieves 73.7% zero-shot ImageNet top1 accuracy, which is on-pair with CLIP-R50×64. Pre-trained models, code, and datasets shall be released to the community. The contributions are summarized as follows:

- To the best of our knowledge, this is the first work to study self-supervision and cross-modal multi-view supervision in the million-scale image-text pre-training task. Our work opens a new direction to fully exploit the intrinsic supervision within the multi-modal data instead of scaling up data naively.
- We propose novel cross-modal Nearest-Neighbor Supervision (NNS) to harness information from other similar pairs. The NNS can also be regarded as a semantic-level augmentation.

[1] View is originally a visual concept. For simplicity, we use the same term for language.

2 RELATED WORK

2.1 PRE-TRAINED MODELS

The critical idea of pre-training is to first extract general knowledge implicitly from the massive amount of data and then transfer the knowledge to versatile downstream tasks (Han et al., 2021). With the transformer architecture (Vaswani et al., 2017), big pre-trained NLP models, such as BERT-series (Devlin et al., 2018; Liu et al., 2019) and GPT-series (Radford et al., 2019; Brown et al., 2020), have dominated this area (Han et al., 2021). Besides the exquisite architecture, the great success comes from the tremendous language data over the Internet and labor-free supervision (Yang et al., 2019; Radford et al., 2019; Devlin et al., 2018) within the language itself. In the field of CV, supervised pre-training on ImageNet is still the standard practice. While achieving great success on downstream CV tasks (Girshick et al., 2014; Long et al., 2015; Vinyals et al., 2015) , this supervised manner is hard to scale. To address this challenge, our DeCLIP learns directly from image-text pairs that are abundant across the Internet. More importantly, by exploiting the widespread supervision within the pairs, our DeCLIP is more data-efficient than the prior art.

2.2 SUPERVISION WITHIN DATA

Language supervision Joulin et al. (2016); Gomez et al. (2017); Zhang et al. (2020); Sariyildiz et al. (2020); Desai & Johnson (2021) demonstrate the effectiveness of learning transferable visual features from language supervision. However, these works are limited to a small dataset such as Flickr (Young et al., 2014) or COCO (Lin et al., 2014). Pioneering work CLIP (Radford et al., 2021) and ALIGN (Jia et al., 2021) achieve prestigious performance via learning from 400M/1B image-text pairs. We are following these two works to improve their data efficiency.

Visual self-supervision Our work is also highly related to self-supervised learning (SSL) (LeCun & Misra, 2021). Contrastive learning, as a pretext task of SSL, has achieved remarkable success in visual representation learning (He et al., 2020; Chen et al., 2020a; Caron et al., 2020; Grill et al., 2020; Chen et al., 2020a). Researchers also extend contrastive learning into multi-modal settings (Yuan et al., 2021). However, it is only limited to a small COCO dataset (Yuan et al., 2021).

Nearest-neighbor supervision Recently, researchers have exploited nearest-neighbor supervision to learn visual features (Dwibedi et al., 2021; Van Gansbeke et al., 2021). They find that using nearest-neighbor as positive samples in the contrastive loss improves the performances on multiple downstream tasks. However, they mainly focus on the single visual modality pretraining on relatively small datasets, such as ImageNet. We propose novel nearest-neighbor supervision for multi-modal learning to harness information from other similar pairs.

2.3 MULTI-MODAL LEARNING

Multi-modal learning aims to build models that can process and relate information from multiple modalities (Baltrušaitis et al., 2018). Vision-language tasks, such as VQA (Antol et al., 2015; Gao et al., 2019), image captioning (Xu et al., 2015), require an understanding of both textual and visual semantics. Most vision-language models use a bunch of cross-modal transformers to fuse and align the information between text and image, such as LXMERT (Tan & Bansal, 2019), UNITER (Chen et al., 2020b), ViLBERT (Lu et al., 2019), VisualBERT (Li et al., 2019), OSCAR (Li et al., 2020), Pixel-BERT (Huang et al., 2020). These methods either need an off-the-shelf object detector to extract region features or dedicated cross-modal transformer layers, significantly hindering their scalability. Our DeCLIP, by contrast, uses a simple yet effective two-tower framework with multi-modal interaction only at the top. Moreover, this series of models (Radford et al., 2021; Jia et al., 2021; Huo et al., 2021) can perform zero-shot recognition, adapting to new categories with no seen labeled data. Shen et al. (2021) also shows that the pre-trained CLIP model can significantly benefit the downstream VQA and image caption tasks. Our DeCLIP is supposed to be compatible with more modalities, e.g., acoustic signals (Akbari et al., 2021). More modalities included, more correlated supervision are expected to be exploited. We hope our DeCLIP can inspire and advance the future study of multi-modal learning.

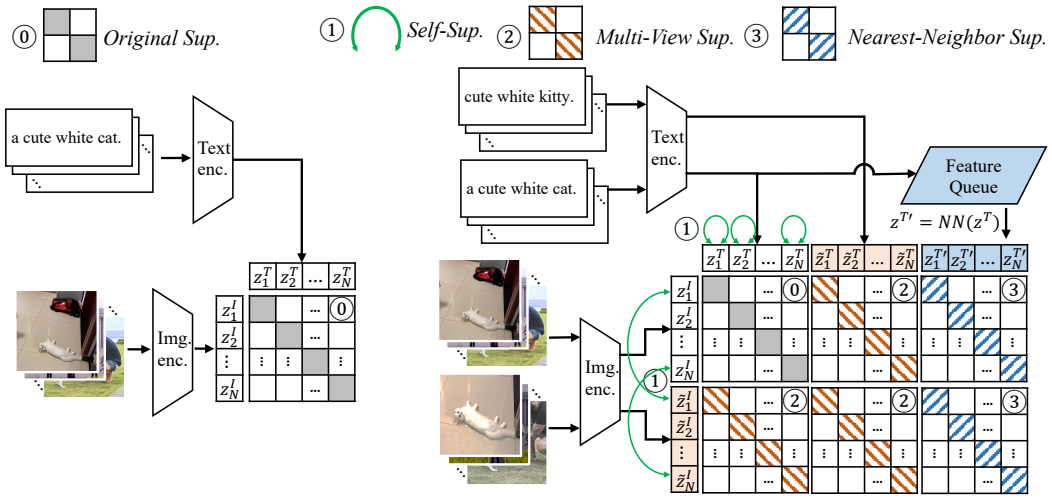

(a) CLIP & ALIGN

(b) DeCLIP

Figure 4: (a) CLIP and ALIGN jointly train an image encoder and a text encoder to predict the correct pairings of a batch of (image, text) training examples. (b) Our DeCLIP overview. ① means Self-Supervision(SS). For image SS, we maximize the similarity between two augmented views of the same instance. For text SS, we leverage Masked Language Modeling(MLM) within a text sentence. ② represents cross-modal Multi-View Supervision(MVS). We first have two augmented views of both image and text, then contrast the 2×2 image-text pairs. ③ indicates Nearest-Neighbor Supervision(NNS). We sample text NN in the embedding space to serve as additional supervision. The combination of the three supervision leads to efficient multi-modal learning.

3 Approach

In this section, we first revisit CLIP and denote some basic concepts, such as image-text contrastive supervision (i.e., the InfoNCE loss). Next, we present the overview of our DeCLIP framework. Then we introduce every auxiliary supervision: Self-Supervision(SS), Multi-View Supervision(MVS), and Nearest-Neighbor Supervision(NNS).

3.1 Revisiting CLIP

Contrastive Language-Image Pre-training (CLIP) (Radford et al., 2021) aims to learn directly from the raw text about images. They use a dual-encoder architecture as in Fig. 4(a). The model consists of an image encoder (e.g., CNN (He et al., 2016) or ViT (Dosovitskiy et al., 2020)) and a text encoder(e.g., Transformer (Vaswani et al., 2017) or its variants (Radford et al., 2019)), with a multimodal interaction at the top. The image and text features are projected to the same dimension and followed by L2 normalization before interaction. At the training phase, a contrastive objective pushes the embeddings of matched image-text pairs together while pushing those of non-matched pairs apart. In a batch of N image-text pairs $\{(\boldsymbol{x}_i^I, \boldsymbol{x}_i^T)\}$, we denote $\boldsymbol{x}_i^I$ and $\boldsymbol{x}_i^T$ as image and text of the i_{th} pair. Let $\boldsymbol{z}_i^I$ and $\boldsymbol{z}_j^T$ be the normalized embedding of the i_{th} image and j_{th} text, respectively. CLIP uses InfoNCE loss (Oord et al., 2018). The loss for the image encoder can be denoted as Eq. 1.

$$L_I = -\frac{1}{N}\sum_{i=1}^{N}\log\frac{\exp(\text{sim}(\boldsymbol{z}_i^I, \boldsymbol{z}_i^T)/\tau)}{\sum_{j=1}^{N}\exp(\text{sim}(\boldsymbol{z}_i^I, \boldsymbol{z}_j^T)/\tau)} \tag{1}$$

Here, the similarity function $\text{sim}(,)$ is measured by dot product, and τ is a learnable temperature variable to scale the logits. We have a symmetrical loss for image and text encoder, thus the overall loss function L_{CLIP} is the average of L_I and L_T.

At the test phase, the learned text encoder synthesizes a zero-shot linear classifier by embedding the arbitrary categories of the test dataset. Because it is rare in the dataset that image caption is just

a single word, CLIP uses prompts to make up the context of the category {`label`}, such as "`a photo of a` {`label`}". Unless otherwise specified, we use the same prompt engineering and ensembling techniques as CLIP. Details can be found in Appendix E.

3.2 Overview of DeCLIP

As shown in Fig. 4(b), our DeCLIP has three additional supervisory signals.

① We first use existing methods to exploit image and text Self-Supervision (SS) within its modality. For image SS, we adopt the simple yet effective SimSiam (Chen & He, 2021). The objective is to maximize the similarity between two augmented image features. For text SS, we adopt the most widely used Masked Language Modeling (MLM) (Devlin et al., 2018) as the pre-text task. We believe other kinds of self-supervised learning algorithms (e.g. MoCo (He et al., 2020), SimCSE (Gao et al., 2021) are orthogonal with our framework.

② While SS only focuses on a single modality, we further propose cross-modal Multi-View Supervision (MVS). We apply stochastic data augmentations for both images and texts, resulting in two correlated views[1] of each example. Then, the image-text contrastive loss is calculated for all the 2×2 pairs. Worth mentioning, the original CLIP does not use text augmentations and only uses random square crop image augmentations, thereby is data-hungry. The extension is instinctive and straightforward. Specifically, we contrast the 2×2 pairs and resulting in $3\times$ more additional supervision.

③ We also propose novel Nearest-Neighbor Supervision (NNS) mined in embedding space to make better use of similar text descriptions among the dataset. In detail, we maintain a first-in-first-out feature queue that is representative of the whole data distribution. We use the nearest-neighbor search in embedding space to get the semantically similar text descriptions. Then we use the image-text contrastive loss to get additional supervision.

3.3 Supervision exists everywhere

Self-Supervision within each modality Following SimSiam (Chen & He, 2021) (depicted in Fig 5(a)), we first have two augmented views (x^I, $\tilde{x}^I$) for each image. These two views are sent to the image encoder (weights are shared between views). We also use the popularized nonlinear predictor module, which is typically a 2-layer MLP, to improve the representation quality in the encoder (Chen et al., 2020a). The objective is to maximize the similarity between $\tilde{z}^I$ and p^I, which is a negative cosine similarity in this paper. To avoid the trivial "collapsing" solution, we follow (Chen & He, 2021) to adopt a stop-grad technique.

As shown in Fig. 5(b), we follow the method in BERT (Devlin et al., 2018) for our text self-supervision. In detail, we first randomly choose 15% of all tokens in each sequence. Then the token is replaced with (1) the `[mask]` token 80% of the time (2) a random token 10% of the time (3) the unchanged token 10% of the time. Then, the output of the language module for the corresponding token is used to predict the original token with cross-entropy loss.

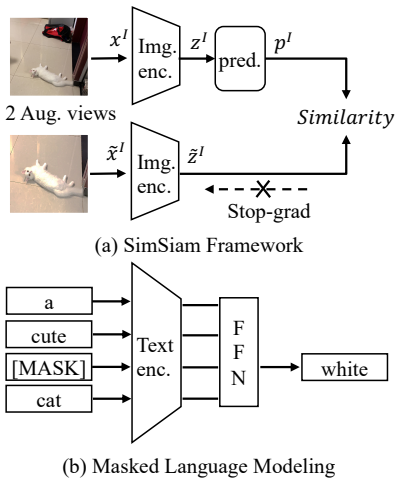

Figure 5: Self-Supervision with each modality. We adopt SimSiam and MLM for image and text SS.

Multi-View Supervision The authors only contrast the original text (w/o augmentation) with a single 'global view' of the image in the original CLIP. However, the text annotation of the image might not describe the whole picture, instead depicts a small local view of this image. For instance, as shown in the image with the text "`a cute white cat`" in Fig. 4, the central concept (cat) only occupies a small part of the picture. To mitigate this discrepancy, we get a closer look at the local region and utilize it as our auxiliary supervision, as shown in the augmented view in Fig. 4(b). This intuitive idea is akin to the successful `Multi-crop` transformation (Caron et al., 2020; Van Gansbeke et al., 2021) in image SSL. We further extend it into the multi-modal

setting. More specifically, we reuse the two image views introduced in SS, which contains the `RandomResizedCrop` policy to obtain a small local view. For text, as our goal is to understand the overall semantic meaning of a sentence, we adopt text classification augmentation EDA (Wei & Zou, 2019) to generate two text views. Besides the original contrastive loss between (z^I, z^T), we can contrast $(z^I, \tilde{z}^T)$, $(\tilde{z}^I, z^T)$ and $(\tilde{z}^I, \tilde{z}^T)$, leading to $3\times$ diverse and high-quality additional supervision. More conveniently, they are naturally compatible with the image-text contrastive loss as denoted in Eq. 1.

Nearest-Neighbor Supervision As shown in Fig 3, one image is likely to have other similar text descriptions among the dataset. To harness the information from other pairs and go beyond single pairs, we propose using nearest-neighbor (NN) to obtain more diverse supervision. More formally, we aim to find the NN feature $z^{T'}$ of text feature z^T in the embedding space. The distance between two features could be measured by a simple cosine similarity. It is infeasible to search NN in the whole million-scale dataset. Thus, we maintain a FIFO queue Q to simulate the whole data distribution. The size of Q is 64K in our implementation. As shown in Fig. 6, we further get the contrastive loss between $(z^I, z^{T'})$. Since there are two augmented image features, we also calculate the contrastive loss between $(\tilde{z}^I, z^{T'})$. Fortunately, NNS is also compatible with Eq. 1.

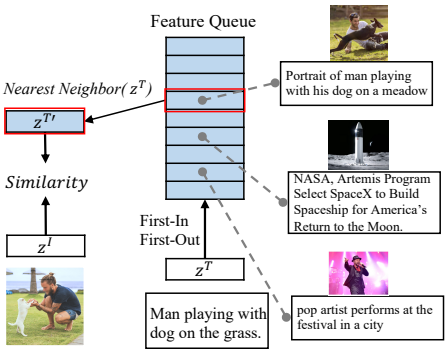

Figure 6: Nearest-Neighbor Supervision. $z^{T'}$ is the NN of feature z^T in the embedding space. $z^{T'}$ will serve as an additional objective for z^I. We use the feature-level nearest neighbor for the text descriptions as the supervision.

In summary, we denote L_{ISS} and L_{TSS} as the loss function of image SS and text SS, respectively. L_{MVS} is multi-view loss, and L_{NNS} is nearest-neighbor loss. We have the overall loss function of our DeCLIP as in Eq. 2.

$$L_{DeCLIP} = (1 - \alpha - \beta - \gamma)L_{CLIP} + \alpha(L_{ISS} + L_{TSS}) + \beta L_{MVS} + \gamma L_{NNS} \tag{2}$$

4 Experiments

4.1 Datasets

Pre-training datasets We summarize our pre-training dataset as in Tab. 1. Our DeCLIP full data consists of two parts: open-source data and web-crawled data. The open-source data comes from three different datasets: Conceptual Captions (CC3M) (Sharma et al., 2018), Conceptual 12M (CC12M) (Changpinyo et al., 2021), and YFCC (Thomee et al., 2016). Worth mentioning, due to the download failure or non-English caption, we do not obtain the complete data for these datasets. We further use the YFCC15M query to crawl about 59M filtered web data on the Internet, together with open-source data to form the 88M DeCLIP full pre-training dataset. More details can be seen in Appendix C.

Table 1: Details of DeCLIP pre-training datasets.

Dataset	Training Size
CLIP (Radford et al., 2021)	400M
ALIGN (Jia et al., 2021)	1.8B
CC (Sharma et al., 2018)	3M
CC-12M (Changpinyo et al., 2021)	11M
YFCC (Thomee et al., 2016)	15M
DeCLIP open-source data	29M
DeCLIP web-crawled data	59M
DeCLIP full data	88M

Downstream datasets We assess our model performances in a wider variety of distributions and tasks. Following the CLIP (Radford et al., 2021), we evaluate the image encoder transferability on 11 widely used downstream datasets, such as Food-101, CIFAR-10, etc. To conduct a fair comparison, the metric and division for each dataset that can be collected are consistent with those of CLIP. More details of downstream datasets can be found in Tabel 6 of Appendix D.

Table 2: Zero-shot top1 accuracy on ImageNet. Our DeCLIP shows great data-efficency.

METHOD	IMAGE ENCODER	# PARAMS	TRAINING SIZE	ZERO-SHOT TOP1 ACC.
CLIP†	RESNET50	24M	88M	56.9
CLIP	RESNET50	24M	400M	59.6
DECLIP	RESNET50	**24M**	**88M(↓ 4.5×)**	**62.5(↑ +2.9)**
CLIP	RESNET101	42M	400M	62.2
CLIP†	VIT-B/32	88M	88M	57.4
CLIP	VIT-B/32	88M	400M	63.2
DECLIP	VIT-B/32	**88M**	**88M(↓ 4.5×)**	**66.2(↑ +3.0)**
CLIP	RESNET50×64	291M	400M	73.6
DECLIP	REGNETY-64GF	**276M**	**88M(↓ 4.5×)**	**73.7(↑ +0.1)**

† OUR REIMPLEMENTATION.

4.2 EXPERIMENTS SETUP

Network architectures Following CLIP, we first consider two different architectures for the image encoder: a modified version of ResNet50 (Radford et al., 2021) and ViT-B/32 (Dosovitskiy et al., 2020). The text encoder is a Transformer (Vaswani et al., 2017) with the architecture modifications described in Radford et al. (2019). The image and text features are projected to the same 1024 dimension, followed by L2 normalization before interaction. Benefiting from the rapid progress of large CV models, we further scale up our model. Our largest model is a RegNetY-64GF (Radosavovic et al., 2020; Goyal et al., 2021) image encoder with a BERT (Devlin et al., 2018) text encoder, which is on-pair with the largest CLIP-R50×64 model.

Pre-training setup For a fair comparison with CLIP, we train our DeCLIP-ResNet50 and DeCLIP-ViT-B/32 from scratch for 32 epochs. Unless otherwise specified, we use full data, i.e., 88M image-text pairs, to obtain the best performance. The input resolution of the image encoder is 224×224, and the maximum context length of the text encoder is 76. The learnable temperature parameter τ is initialized to 0.07. The loss weights of additional supervision α, β and γ are all set to 0.2. More details can be found in Appendix C.

Downstream evaluation setup We evaluate our model transferability by performing linear classification on frozen features, i.e., the pre-trained image encoder is fixed and serves as a feature extractor. After feature extraction, we train the linear classifier with the L-BFGS optimizer as the same in Radford et al. (2021).

4.3 MAIN RESULTS

Zero-shot recognition on ImageNet After pre-training, we use natural language to refer to visual concepts enabling the zero-shot ability of our model. As shown in Fig. 1, our DeCLIP-ResNet50 consistently outperforms the CLIP-ResNet50 across all dataset sizes. When the data amount reaches 56M (29M open-source + 27M web-crawled), our model can achieve 60.4% accuracy, 0.8% above the CLIP-ResNet50, while using 7.1× fewer data. As described in Tab. 2, with our full data, our best ResNet50/ViT-B32 models boost the zero-shot performance to 62.5% and 66.2%, nearly 3.0% higher than the best number reported for these two architectures. Moreover, our DeCLIP-ResNet50 is even 0.3% better than CLIP-ResNet101, revealing the effectiveness and efficiency of our framework. Scaling up model capacity works in our framework as well. Our biggest DeCLIP-RegNetY-64GF achieves 73.7% accuracy, which is 0.1% above CLIP ResNet50×64 with fewer parameters.

Downstream evaluation results We report our linear probe performance on 11 downstream datasets in Tab. 3. Our DeCLIP-ResNet50 outperforms its CLIP counterpart in 8 out of 11 datasets, with a 0.8% average improvement. There are some datasets that our models perform worse than CLIP models, such as SUN and Food101. We conjecture that this is caused by the different distribution of the pre-trained dataset. Interestingly, our ResNet50 and ViT-B/32 models might have distinct performance on several datasets, such as Pets and Aircraft. We infer that these two types

Table 3: Linear probe performance on 11 downstream datasets. There are some abbreviations. C10/100 is CIFAR10/100. F101 is Food101. Flow is Flowers. Cal is Caltech. Air is Aircraft. IN is ImageNet. Our DeCLIP models achieve higher average accuracy over 11 datasets.

MODEL	PETS	C10	C100	SUN	F101	FLOW.	CARS	CAL.	AIR.	DTD	IN	AVG.
CLIP-RESNET50†	85.1	87.3	65.0	71.3	80.8	98.2	77.2	89.6	44.8	71.0	70.8	76.5
CLIP-RESNET50	88.2	88.7	70.3	**73.3**	**86.4**	96.1	78.3	89.6	**49.1**	76.4	73.3	79.1
DECLIP-RESNET50	**88.7**	**89.8**	**71.2**	72.8	82.7	**99.2**	**81.7**	**93.9**	48.4	**76.8**	**74.0**	**79.9**(↑ **+0.8**)
CLIP-VIT-B/32†	85.3	91.6	74.2	72.3	80.8	97.9	77.6	93.2	47.0	72.5	70.3	78.4
CLIP-VIT-B/32	**90.0**	95.1	80.5	**76.6**	**88.8**	96.9	**81.8**	93.0	52.0	76.5	**76.1**	82.5
DECLIP-VIT-B/32	89.2	**96.5**	**84.7**	75.0	85.0	**99.1**	81.6	**94.8**	**53.5**	**78.5**	75.3	**83.0** (↑ **+0.5**)

† OUR REIMPLEMENTATED CLIP MODEL TRAINED ON 88M DATA.

Table 4: Ablation on additional supervision. SS/MVS/NNS denotes Self-Supervision, Multi-View Supervision and Nearest-Neighbor Supervision, respectively.

CLIP	MVS	SS	NNS	ZERO-SHOT
✓	×	×	×	20.6
✓	✓	×	×	24.8(↑ +4.2)
✓	✓	✓	×	25.4(↑ +4.8)
✓	✓	✓	✓	**27.2**(↑ **+6.6**)

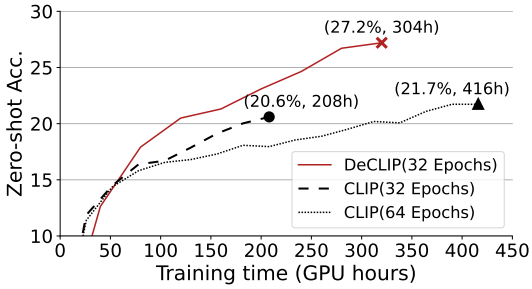

Figure 7: Ablation on pre-training cost on CC3M dataset. The proposed method performs better with less training time.

of neural networks might have different data preferences, i.e., different feature extraction capacities when they meet the same data.

4.4 ABLATION STUDY

Ablation on additional supervision In order to understand the effectiveness of each additional supervision, we conduct an ablation study as indicated in Tab. 4. We follow the DeCLIP-ResNet50 protocol in the pre-training setup except for a smaller 1024 batch size on a smaller CC3M dataset. The single image-text contrastive supervision (CLIP) results in 20.6% zero-shot top1 accuracy on ImageNet. We can observe that MVS boost amazing 4.2% improvement over the original CLIP. As discussed in Sec. 3.3, the benefits might come from two sides: 1). the MVS can look at a small local view of an image which might be a better fit with the text description. 2). 2×2 augmented views can provide $3\times$ diverse and high-quality additional supervision, thus leading to more robust representations. SS can further contribute an additional 0.6% improvement on the basis of MVS. We believe SS could bring more improvements with proper dedicated SSL methods. NNS further brings 1.8% improvement on the high basis of SS. We will discuss more about NNS at Sec. 4.5. On the YFCC15M dataset, our DeCLIP using full additional supervision gets significant effect improvement, Appendix F shows the details.

Ablation on training cost Since we need to encode twice for each image-text pair, we admit our DeCLIP needs a higher training cost than CLIP. Regarding the training time, one DeCLIP iteration equals $1.5\times$ CLIP iteration. In this ablation, we train the original CLIP-ResNet50 longer than our DeCLIP-ResNet50. As shown in Fig. 7, longer 64 epochs training can bring about 1.1% improvement. However, our model has 27.2% top1 accuracy, which is still 5.3% higher than the time-equivalent CLIP. It reveals that our framework can extract richer and more representative features through our proposed supervision. We also include memory usage ablation in Appendix F.

4.5 ANALYSIS

Class activation maps We try to understand what renders our DeCLIP effective. As shown in Fig. 8, we visualize the class activation maps (CAM) (Zhou et al., 2016) of different models trained

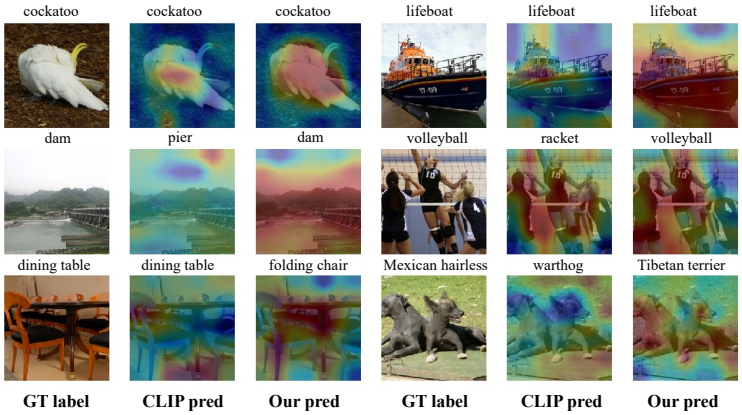

Figure 8: Class activation maps (CAM) for the CLIP vs. our DeCLIP model trained on the YFCC dataset. The CAMs of our model segment the complete object, while the CLIP model only looks at a few components.

Figure 9: Nearest neighbor samples from different datasets. As we can see, the NN pair is very similar to the original pair, thus it can provide high-quality supervision.

on the YFCC dataset. The results validate that the proposed method learns more representative features with the aid of multiple supervision.

Nearest neighbor samples In Fig 9, we show some nearest neighbor (NN) samples from different datasets. The first row is the original image-text pair, while the second row is the NN pair. In general, we can see that the texts have similar intellectual meanings. Therefore, the NN pair can provide high-quality supervision. When taking datasets into consideration, the matching performs very well in well-filtered datasets, such as CC3M and CC12M. This matching might be a little worse in more noisy datasets, such as YFCC and web-crawled, but it can still provide some beneficial guidance.

5 Conclusion

This paper introduces DeCLIP, a Data efficient Contrastive Language-Image Pre-training paradigm. Our goal is to learn visual representations through the use of broader and scalable supervision. Specifically, instead of using the single image-text contrastive supervision, we fully exploit data potential through the use of (1) self-supervision within each modality; (2) multi-view supervision across modalities; (3) nearest-neighbor supervision from other similar pairs. Experimentally, DeCLIP shows superior effectiveness and efficiency with different types of neural nets(CNN and ViT) and different amounts of data. We hope our work could bring insights about exploiting the multi-modal data.

REFERENCES

Hassan Akbari, Linagzhe Yuan, Rui Qian, Wei-Hong Chuang, Shih-Fu Chang, Yin Cui, and Boqing Gong. Vatt: Transformers for multimodal self-supervised learning from raw video, audio and text. *arXiv preprint arXiv:2104.11178*, 2021.

Stanislaw Antol, Aishwarya Agrawal, Jiasen Lu, Margaret Mitchell, Dhruv Batra, C Lawrence Zitnick, and Devi Parikh. Vqa: Visual question answering. In *Proceedings of the IEEE international conference on computer vision*, pp. 2425–2433, 2015.

Tadas Baltrušaitis, Chaitanya Ahuja, and Louis-Philippe Morency. Multimodal machine learning: A survey and taxonomy. *IEEE transactions on pattern analysis and machine intelligence*, 41(2): 423–443, 2018.

Tom B Brown, Benjamin Mann, Nick Ryder, Melanie Subbiah, Jared Kaplan, Prafulla Dhariwal, Arvind Neelakantan, Pranav Shyam, Girish Sastry, Amanda Askell, et al. Language models are few-shot learners. *arXiv preprint arXiv:2005.14165*, 2020.

Mathilde Caron, Ishan Misra, Julien Mairal, Priya Goyal, Piotr Bojanowski, and Armand Joulin. Unsupervised learning of visual features by contrasting cluster assignments. *arXiv preprint arXiv:2006.09882*, 2020.

Soravit Changpinyo, Piyush Sharma, Nan Ding, and Radu Soricut. Conceptual 12m: Pushing web-scale image-text pre-training to recognize long-tail visual concepts. In *Proceedings of the IEEE/CVF Conference on Computer Vision and Pattern Recognition*, pp. 3558–3568, 2021.

Ting Chen, Simon Kornblith, Mohammad Norouzi, and Geoffrey Hinton. A simple framework for contrastive learning of visual representations. In *International conference on machine learning*, pp. 1597–1607. PMLR, 2020a.

Xinlei Chen and Kaiming He. Exploring simple siamese representation learning. In *Proceedings of the IEEE/CVF Conference on Computer Vision and Pattern Recognition*, pp. 15750–15758, 2021.

Yen-Chun Chen, Linjie Li, Licheng Yu, Ahmed El Kholy, Faisal Ahmed, Zhe Gan, Yu Cheng, and Jingjing Liu. Uniter: Universal image-text representation learning, 2020b.

Jia Deng, Wei Dong, Richard Socher, Li-Jia Li, Kai Li, and Li Fei-Fei. Imagenet: A large-scale hierarchical image database. In *2009 IEEE conference on computer vision and pattern recognition*, pp. 248–255. Ieee, 2009.

Karan Desai and Justin Johnson. Virtex: Learning visual representations from textual annotations. In *Proceedings of the IEEE/CVF Conference on Computer Vision and Pattern Recognition*, pp. 11162–11173, 2021.

Jacob Devlin, Ming-Wei Chang, Kenton Lee, and Kristina Toutanova. Bert: Pre-training of deep bidirectional transformers for language understanding. *arXiv preprint arXiv:1810.04805*, 2018.

Alexey Dosovitskiy, Lucas Beyer, Alexander Kolesnikov, Dirk Weissenborn, Xiaohua Zhai, Thomas Unterthiner, Mostafa Dehghani, Matthias Minderer, Georg Heigold, Sylvain Gelly, et al. An image is worth 16x16 words: Transformers for image recognition at scale. *arXiv preprint arXiv:2010.11929*, 2020.

Debidatta Dwibedi, Yusuf Aytar, Jonathan Tompson, Pierre Sermanet, and Andrew Zisserman. With a little help from my friends: Nearest-neighbor contrastive learning of visual representations. *arXiv preprint arXiv:2104.14548*, 2021.

Peng Gao, Zhengkai Jiang, Haoxuan You, Pan Lu, Steven CH Hoi, Xiaogang Wang, and Hongsheng Li. Dynamic fusion with intra-and inter-modality attention flow for visual question answering. In *Proceedings of the IEEE/CVF Conference on Computer Vision and Pattern Recognition*, pp. 6639–6648, 2019.

Tianyu Gao, Xingcheng Yao, and Danqi Chen. Simcse: Simple contrastive learning of sentence embeddings. *arXiv preprint arXiv:2104.08821*, 2021.

Ross Girshick, Jeff Donahue, Trevor Darrell, and Jitendra Malik. Rich feature hierarchies for accurate object detection and semantic segmentation. In *Proceedings of the IEEE conference on computer vision and pattern recognition*, pp. 580–587, 2014.

Lluis Gomez, Yash Patel, Marçal Rusiñol, Dimosthenis Karatzas, and CV Jawahar. Self-supervised learning of visual features through embedding images into text topic spaces. In *Proceedings of the IEEE Conference on Computer Vision and Pattern Recognition*, pp. 4230–4239, 2017.

Priya Goyal, Mathilde Caron, Benjamin Lefaudeux, Min Xu, Pengchao Wang, Vivek Pai, Mannat Singh, Vitaliy Liptchinsky, Ishan Misra, Armand Joulin, et al. Self-supervised pretraining of visual features in the wild. *arXiv preprint arXiv:2103.01988*, 2021.

Jean-Bastien Grill, Florian Strub, Florent Altché, Corentin Tallec, Pierre H Richemond, Elena Buchatskaya, Carl Doersch, Bernardo Avila Pires, Zhaohan Daniel Guo, Mohammad Gheshlaghi Azar, et al. Bootstrap your own latent: A new approach to self-supervised learning. *arXiv preprint arXiv:2006.07733*, 2020.

Xu Han, Zhengyan Zhang, Ning Ding, Yuxian Gu, Xiao Liu, Yuqi Huo, Jiezhong Qiu, Liang Zhang, Wentao Han, Minlie Huang, et al. Pre-trained models: Past, present and future. *AI Open*, 2021.

Kaiming He, Xiangyu Zhang, Shaoqing Ren, and Jian Sun. Deep residual learning for image recognition. In *Proceedings of the IEEE conference on computer vision and pattern recognition*, pp. 770–778, 2016.

Kaiming He, Haoqi Fan, Yuxin Wu, Saining Xie, and Ross Girshick. Momentum contrast for unsupervised visual representation learning. In *Proceedings of the IEEE/CVF Conference on Computer Vision and Pattern Recognition*, pp. 9729–9738, 2020.

Zhicheng Huang, Zhaoyang Zeng, Bei Liu, Dongmei Fu, and Jianlong Fu. Pixel-bert: Aligning image pixels with text by deep multi-modal transformers. *arXiv preprint arXiv:2004.00849*, 2020.

Yuqi Huo, Manli Zhang, Guangzhen Liu, Haoyu Lu, Yizhao Gao, Guoxing Yang, Jingyuan Wen, Heng Zhang, Baogui Xu, Weihao Zheng, et al. Wenlan: Bridging vision and language by large-scale multi-modal pre-training. *arXiv preprint arXiv:2103.06561*, 2021.

Chao Jia, Yinfei Yang, Ye Xia, Yi-Ting Chen, Zarana Parekh, Hieu Pham, Quoc V Le, Yunhsuan Sung, Zhen Li, and Tom Duerig. Scaling up visual and vision-language representation learning with noisy text supervision. *arXiv preprint arXiv:2102.05918*, 2021.

Armand Joulin, Laurens Van Der Maaten, Allan Jabri, and Nicolas Vasilache. Learning visual features from large weakly supervised data. In *European Conference on Computer Vision*, pp. 67–84. Springer, 2016.

Simon Kornblith, Jonathon Shlens, and Quoc V Le. Do better imagenet models transfer better? In *Proceedings of the IEEE/CVF Conference on Computer Vision and Pattern Recognition*, pp. 2661–2671, 2019.

Alex Krizhevsky, Ilya Sutskever, and Geoffrey E Hinton. Imagenet classification with deep convolutional neural networks. *Advances in neural information processing systems*, 25:1097–1105, 2012.

Y LeCun and I Misra. Self-supervised learning: The dark matter of intelligence, 2021.

Liunian Harold Li, Mark Yatskar, Da Yin, Cho-Jui Hsieh, and Kai-Wei Chang. Visualbert: A simple and performant baseline for vision and language. *arXiv preprint arXiv:1908.03557*, 2019.

Xiujun Li, Xi Yin, Chunyuan Li, Pengchuan Zhang, Xiaowei Hu, Lei Zhang, Lijuan Wang, Houdong Hu, Li Dong, Furu Wei, et al. Oscar: Object-semantics aligned pre-training for vision-language tasks. In *European Conference on Computer Vision*, pp. 121–137. Springer, 2020.

Tsung-Yi Lin, Michael Maire, Serge Belongie, James Hays, Pietro Perona, Deva Ramanan, Piotr Dollár, and C Lawrence Zitnick. Microsoft coco: Common objects in context. In *European conference on computer vision*, pp. 740–755. Springer, 2014.

Yinhan Liu, Myle Ott, Naman Goyal, Jingfei Du, Mandar Joshi, Danqi Chen, Omer Levy, Mike Lewis, Luke Zettlemoyer, and Veselin Stoyanov. Roberta: A robustly optimized bert pretraining approach. *arXiv preprint arXiv:1907.11692*, 2019.

Jonathan Long, Evan Shelhamer, and Trevor Darrell. Fully convolutional networks for semantic segmentation. In *Proceedings of the IEEE conference on computer vision and pattern recognition*, pp. 3431–3440, 2015.

Jiasen Lu, Dhruv Batra, Devi Parikh, and Stefan Lee. Vilbert: Pretraining task-agnostic visiolinguistic representations for vision-and-language tasks. *arXiv preprint arXiv:1908.02265*, 2019.

George A Miller. Wordnet: a lexical database for english. *Communications of the ACM*, 38(11): 39–41, 1995.

Aaron van den Oord, Yazhe Li, and Oriol Vinyals. Representation learning with contrastive predictive coding. *arXiv preprint arXiv:1807.03748*, 2018.

Alec Radford, Jeffrey Wu, Rewon Child, David Luan, Dario Amodei, Ilya Sutskever, et al. Language models are unsupervised multitask learners. *OpenAI blog*, 1(8):9, 2019.

Alec Radford, Jong Wook Kim, Chris Hallacy, Aditya Ramesh, Gabriel Goh, Sandhini Agarwal, Girish Sastry, Amanda Askell, Pamela Mishkin, Jack Clark, et al. Learning transferable visual models from natural language supervision. *arXiv preprint arXiv:2103.00020*, 2021.

Ilija Radosavovic, Raj Prateek Kosaraju, Ross Girshick, Kaiming He, and Piotr Dollár. Designing network design spaces. In *Proceedings of the IEEE/CVF Conference on Computer Vision and Pattern Recognition*, pp. 10428–10436, 2020.

Mert Bulent Sariyildiz, Julien Perez, and Diane Larlus. Learning visual representations with caption annotations. In *Computer Vision–ECCV 2020: 16th European Conference, Glasgow, UK, August 23–28, 2020, Proceedings, Part VIII 16*, pp. 153–170. Springer, 2020.

Piyush Sharma, Nan Ding, Sebastian Goodman, and Radu Soricut. Conceptual captions: A cleaned, hypernymed, image alt-text dataset for automatic image captioning. In *Proceedings of ACL*, 2018.

Sheng Shen, Liunian Harold Li, Hao Tan, Mohit Bansal, Anna Rohrbach, Kai-Wei Chang, Zhewei Yao, and Kurt Keutzer. How much can clip benefit vision-and-language tasks? *arXiv preprint arXiv:2107.06383*, 2021.

Karen Simonyan and Andrew Zisserman. Very deep convolutional networks for large-scale image recognition. *arXiv preprint arXiv:1409.1556*, 2014.

Hao Tan and Mohit Bansal. Lxmert: Learning cross-modality encoder representations from transformers. *arXiv preprint arXiv:1908.07490*, 2019.

Bart Thomee, David A Shamma, Gerald Friedland, Benjamin Elizalde, Karl Ni, Douglas Poland, Damian Borth, and Li-Jia Li. Yfcc100m: The new data in multimedia research. *Communications of the ACM*, 59(2):64–73, 2016.

Wouter Van Gansbeke, Simon Vandenhende, Stamatios Georgoulis, and Luc Van Gool. Revisiting contrastive methods for unsupervised learning of visual representations. *arXiv preprint arXiv:2106.05967*, 2021.

Ashish Vaswani, Noam Shazeer, Niki Parmar, Jakob Uszkoreit, Llion Jones, Aidan N Gomez, Łukasz Kaiser, and Illia Polosukhin. Attention is all you need. In *Advances in neural information processing systems*, pp. 5998–6008, 2017.

Oriol Vinyals, Alexander Toshev, Samy Bengio, and Dumitru Erhan. Show and tell: A neural image caption generator. In *Proceedings of the IEEE conference on computer vision and pattern recognition*, pp. 3156–3164, 2015.

Jason Wei and Kai Zou. Eda: Easy data augmentation techniques for boosting performance on text classification tasks. *arXiv preprint arXiv:1901.11196*, 2019.

Zhirong Wu, Yuanjun Xiong, Stella X Yu, and Dahua Lin. Unsupervised feature learning via non-parametric instance discrimination. In *Proceedings of the IEEE conference on computer vision and pattern recognition*, pp. 3733–3742, 2018.

Kelvin Xu, Jimmy Ba, Ryan Kiros, Kyunghyun Cho, Aaron Courville, Ruslan Salakhudinov, Rich Zemel, and Yoshua Bengio. Show, attend and tell: Neural image caption generation with visual attention. In *International conference on machine learning*, pp. 2048–2057. PMLR, 2015.

Zhilin Yang, Zihang Dai, Yiming Yang, Jaime Carbonell, Russ R Salakhutdinov, and Quoc V Le. Xlnet: Generalized autoregressive pretraining for language understanding. *Advances in neural information processing systems*, 32, 2019.

Peter Young, Alice Lai, Micah Hodosh, and Julia Hockenmaier. From image descriptions to visual denotations: New similarity metrics for semantic inference over event descriptions. *Transactions of the Association for Computational Linguistics*, 2:67–78, 2014.

Xin Yuan, Zhe Lin, Jason Kuen, Jianming Zhang, Yilin Wang, Michael Maire, Ajinkya Kale, and Baldo Faieta. Multimodal contrastive training for visual representation learning. In *Proceedings of the IEEE/CVF Conference on Computer Vision and Pattern Recognition*, pp. 6995–7004, 2021.

Yuhao Zhang, Hang Jiang, Yasuhide Miura, Christopher D Manning, and Curtis P Langlotz. Contrastive learning of medical visual representations from paired images and text. *arXiv preprint arXiv:2010.00747*, 2020.

Bolei Zhou, Aditya Khosla, Agata Lapedriza, Aude Oliva, and Antonio Torralba. Learning deep features for discriminative localization. In *Proceedings of the IEEE conference on computer vision and pattern recognition*, pp. 2921–2929, 2016.

A PSEUDO CODE OF DECLIP

The training pseudo code of DeCLIP is as follows:

Algorithm 1 DeCLIP

Input: $I, \tilde{I}, T, \tilde{T}, image_encoder, text_encoder, Feature_Queue$

function BATCH-UPDATING($I, \tilde{I}, T, \tilde{T}$)
  # Get The Features of The Current Batch.
  $I_f, \tilde{I}_f \leftarrow image_encoder(I), image_encoder(\tilde{I})$
  $T_f, \tilde{T}_f \leftarrow text_encoder(T), text_encoder(\tilde{T})$
  $T_{NN} \leftarrow$ NEAREST-NEIGHBOR($Feature_Queue, T_f$)

  # Calculate The losses.
  $L_{CLIP} \leftarrow$ INFONCE-LOSS(I_f, T_f)
  $L_{SS} \leftarrow$ IMAGE-SS-LOSS($I_f, \tilde{I}_f$) + TEXT-SS-LOSS(T_f)
  $L_{MVS} \leftarrow$ INFONCE-LOSS($I_f, \tilde{T}_f$) + INFONCE-LOSS($\tilde{I}_f, T_f$) + INFONCE-LOSS($\tilde{I}_f, \tilde{T}_f$)
  $L_{NNS} \leftarrow$ INFONCE-LOSS($\tilde{I}_f, \tilde{T}_{NN}$)
  $L_{DeCLIP} \leftarrow (1-\alpha-\beta-\gamma)L_{CLIP} + \alpha L_{SS} + \beta L_{MVS} + \gamma L_{NNS}$

  # Update The Network.
  $image_encoder \leftarrow$ BACKWARD-UPDATE($image_encoder, L_{DeCLIP}$)
  $text_encoder \leftarrow$ BACKWARD-UPDATE($text_encoder, L_{DeCLIP}$)
  $Feature_Queue \leftarrow$ FIFO-UPDATE($Feature_Queue, T_f$)
end function

function IMAGE-SS-LOSS($I_f, \tilde{I}_f$)
  $z, \tilde{z} \leftarrow image_encoder.proj(I_f), image_encoder.proj(\tilde{I}_f)$
  $p, \tilde{p} \leftarrow image_encoder.pred(z), image_encoder.pred(\tilde{z})$
  $z, \tilde{z} \leftarrow z.detach(), \tilde{z}.detach()$
  # Calculate the Negative Cosine Similarity loss.
  $L_{Image-SS} \leftarrow NCS(p, \tilde{z})/2 + NCS(\tilde{p}, z)/2$
  return $L_{Image-SS}$
end function

function TEXT-SS-LOSS(T_f)
  # Get The Masking GT when performing the text-encoder.
  $W_f, W_{gt} \leftarrow T_f.word_feat, T_f.mask_id$
  $W_{pred} \leftarrow text_encoder.pred(W_f)$
  # Calculate the Cross-Entropy loss.
  $L_{Text-SS} \leftarrow CE(W_{gt}, W_{pred})$
  return $L_{Text-SS}$
end function

B DATA AUGMENTATION

Details of SS The image SS uses SimSiam (Chen & He, 2021) method as the image self-supervision. The prediction module is a 2-layer MLP, in which the hidden dimensions are 512 and output dimensions are 1024, the projection module is a 3-layer MLP, in which the hidden and output dimensions are both 1024. The text SS uses the Masked Language Model (Devlin et al., 2018) as the pretext task. In detail, we first randomly choose 15% of all tokens in each sequence. Then the token is replaced with (1) the `[mask]` token 80% of the time (2) a random token 10% of the time (3) the unchanged token 10% of the time.

Image augmentations The augmentation policy includes: `RandomResizedCrop` with scale in [0.2,1.0] (Wu et al., 2018), `ColorJitter` containing {brightness, contrast, saturation, hue}

strength of $\{0.4, 0.4, 0.4, 0.1\}$ with an applying probability of 0.8, `RandomGrayscale` with an applying probability of 0.2. Blurring augmentation (Chen et al., 2020a) has a Gaussian kernel with std in [0.1, 2.0], and `RandomHorizontalFlip`.

Text augmentations We use the EDA (Wei & Zou, 2019) method as our text augmentation strategy, which contains three types of text augmentation strategies: synonym replacement, random swap, and random deletion. Each text will randomly select one of these three types for text augmentation.

C PRE-TRAINING DATASETS & IMPLEMENTATION DETAILS

Open-source data. Conceptual Captions (Sharma et al., 2018) is a 3.3 M image caption open-source data. Due to the failure of the download link, we only download about 3M data(CC3M). Conceptual 12M (Sharma et al., 2018) contains approximately 12M of image-text pairs(CC12M), which is larger than the CC3M and covers a more diverse set of visual concepts. Also, due to the failure of the download link, we only download about 11M data. YFCC (Thomee et al., 2016), the Yahoo Flickr Creative Commons 100M data, is a dataset for vision language tasks. We download about 86.5M data from the YFCC website and use four filtering rules to filter the DeCLIP YFCC15M dataset to benchmark against CLIP YFCC15M. The four rules are: filtering data with damaged images, filtering data without the caption, filtering data with a caption English word ratio less than 0.8, filtering data with a caption only including one part of speech.

Web-crawled data. We use the user tags and machine tags of YFCC15M to form a tag list, and use WordNet (Miller, 1995) to find synonyms for each tag in the tag list to form a synonym tag list. The tag list and synonym tag list form a query list. Then we use the query list to crawl images from the Internet, after filtering data with smaller images, filtering data with damaged images, filtering data without the caption, and filtering data with Chinese in the caption, we collect 59M web crawled data. Tabel 5 shows the source link of pre-training datasets, and Figure 10 shows some cases random sampled from each dataset.

Table 5: The source link of DeCLIP pre-training datasets.

DATASET	DATASET API
CONCEPTUALCAPTIONS	HTTPS://AI.GOOGLE.COM/RESEARCH/CONCEPTUALCAPTIONS
CONCEPTUAL12M	HTTPS://GITHUB.COM/GOOGLE-RESEARCH-DATASETS/CONCEPTUAL-12M
YFCC	HTTP://PROJECTS.DFKI.UNI-KL.DE/YFCC100M
GOOGLE	HTTPS://WWW.GOOGLE.COM.HK

Implementation details We train DeCLIP-ResNet50 (abbr. as R50) and DeCLIP-ViT-B/32 (abbr. as V-B32) from scratch for 32 epochs. For R50, we use the FP16-SGD optimizer with the batch size of 10,240 (128×80). Starting with an 0.01 learning rate (lr), we first linearly increasing the lr to 0.2 (a.k.a warm-up) in one epoch. Then we use cosine anneal lr decay to decrease the lr. The weight decay is set to 0.0001. For V-B32, we use a hybrid FP16-AdamW-SGD optimizer with bacth size 10,240(128×80). For the ViT image encoder, we use AdamW optimizer with the lr warming up from 1e-4 to 1e-3 in one epoch. The weight decay is set to 0.05. For the text encoder, we use the SGD optimizer with the lr warming up from 1e-3 to 0.02 in one epoch. The weight decay is set to 1e-4.

Pre-training cost Our R50 and V-B32 took 8/10 days to train on 80 V100 GPUs, respectively. Our largest DeCLIP-RegNetY-64GF took 21 days on 160 V100 GPUs, while the largest CLIP-R50$\times$64 from (Radford et al., 2021) spent 18 days on 592 V100 GPUs.

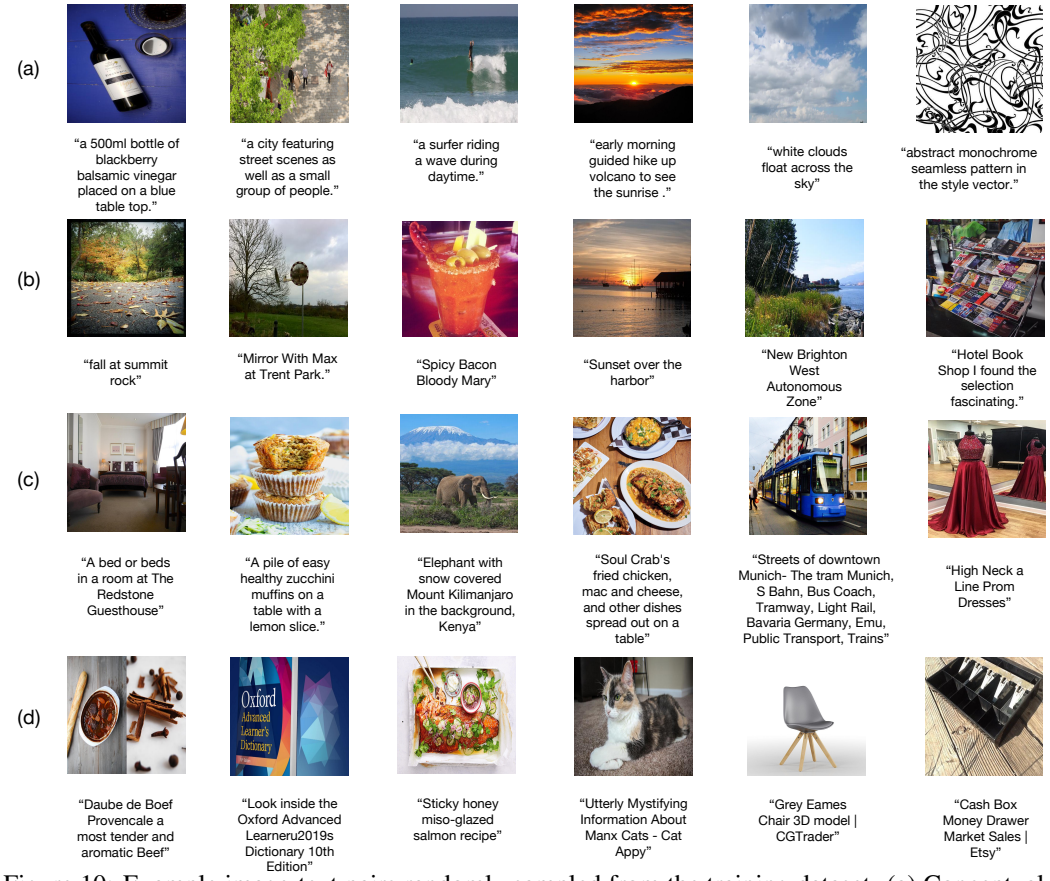

Figure 10: Example image-text pairs randomly sampled from the training dataset. (a) Conceptual Captions, (b) YFCC, (c) Conceptual 12M, (d) Web-crawled.

D DOWNSTREAM DATASETS & IMPLEMENTATION DETAILS

Downstream data. We begin with the 12 datasets from the well-studied evaluation suite introduced by Kornblith et al. (2019). Within these 12 datasets, Birdsnap can not be downloaded, and PASCAL VOC 2007 classification is replaced by more challenging ImageNet-1K, resulting in our 11 datasets. They are: Food-101, CIFAR-10, CIFAR-100, SUN397, Stanford Cars, FGVC Aircraft, Describable Textures, Oxford-IIIT Pets, Caltech-101, Oxford Flowers 102. Tab. 6 is the detailed information of these datasets.

Table 6: Details of DeCLIP downstream datasets.

DATASET	CLASSES	TRAIN SIZE	TEST SIZE	EVALUATION METRIC
CIFAR10	10	50,000	10,000	ACCURACY
CIFAR100	100	50,000	10,000	ACCURACY
FOOD-101	101	75,750	25,250	ACCURACY
OXFORDIIIT-PETS	37	3,680	3,669	MEAN PER CLASS
OXFORD 102 FLOWERS	102	2,040	6,149	MEAN PER CLASS
SUN	397	19,850	19,850	ACCURACY
STANFORD CARS	196	8,144	8,041	ACCURACY
DTD	47	3,760	1,880	ACCURACY
CALTECH-101	102	3,060	6,085	MEAN PER
FGVC AIRCRAFT	100	6,667	3,333	MEAN PER CLASS
IMAGENET1K	1000	1,281,167	50,000	ACCURACY

Implementation details We follow CLIP (Radford et al., 2021) to train a logistic regression classifier using L-BFGS, with maximum 1,000 iterations, and report the corresponding metric for each dataset. We determine the L2 regularization strength λ using a hyperparameter sweep on the validation sets over the range between 10^{-6} and 10^{6}, with 96 logarithmically spaced steps. To save compute required for the sweeps, we perform a parametric binary search that starts with $\lambda = [10^{-6}, 10^{-4}, 10^{-2}, 1, 10^{2}, 10^{4}, 10^{6}]$ and iteratively halves the interval around the peak until it reaches a resolution of 8 steps per decade. The hyperparameter sweeps are performed on a validation split of each dataset. For the datasets that contains a validation split in addition to from the test split, we use the provided validation set to perform the hyperparameter search, and for the datasets that do not provide a validation split or have not published labels for the test data, we split the training dataset to perform the hyperparameter search and report the performance on the validation data.

E PROMPT ENGINEERING

Due to the reason that it's relatively rare in the dataset for the text to be a single word, we use prompts such as `"a photo of a {label}"` for zero-shot classification. For a fair comparison, we use the same prompts as proposed in Radford et al. (2021) for the ImageNet dataset. As shown in Fig 11, the prompts reduce the domain gap between the training dataset and testset, and fully consider the different situations for the picture.

a bad photo of a {label}.	a close-up photo of a {label}.	the origami {label}.	a jpeg corrupted photo of the {labe
a photo of many {label}.	a black and white photo of the {label}.	the {label} in a video game.	a good photo of a {label}.
a sculpture of a {label}.	a painting of the {label}.	a sketch of a {label}.	a plushie {label}.
a photo of the hard to see {label}.	a painting of a {label}.	a doodle of the {label}.	a photo of the nice {label}.
a low resolution photo of the {label}.	a pixelated photo of the {label}.	a origami {label}.	a photo of the small {label}.
a rendering of a {label}.	a sculpture of the {label}.	a low resolution photo of a {label}.	a photo of the weird {label}.
graffiti of a {label}.	a bright photo of the {label}.	the toy {label}.	the cartoon {label}.
a bad photo of the {label}.	a cropped photo of a {label}.	a rendition of the {label}.	art of the {label}.
a cropped photo of the {label}.	a plastic {label}.	a photo of the clean {label}.	a drawing of the {label}.
a tattoo of a {label}.	a photo of the dirty {label}.	a photo of a large {label}.	a photo of the large {label}.
the embroidered {label}.	a jpeg corrupted photo of a {label}.	a rendition of a {label}.	a black and white photo of a {label
a photo of a hard to see {label}.	a blurry photo of the {label}.	a photo of a nice {label}.	the plushie {label}.
a bright photo of a {label}.	a photo of the {label}.	a photo of a weird {label}.	a dark photo of a {label}.
a photo of a clean {label}.	a good photo of the {label}.	a blurry photo of a {label}.	itap of a {label}.
a photo of a dirty {label}.	a rendering of the {label}.	a cartoon {label}.	graffiti of the {label}.
a dark photo of the {label}.	a {label} in a video game.	art of a {label}.	a toy {label}.
a drawing of a {label}.	a photo of one {label}.	a sketch of the {label}.	itap of my {label}.
a photo of my {label}.	a doodle of a {label}.	a embroidered {label}.	a photo of a cool {label}.
the plastic {label}.	a close-up photo of the {label}.	a pixelated photo of a {label}.	a photo of a small {label}.
a photo of the cool {label}.	a photo of a {label}.	itap of the {label}.	a tattoo of the {label}.

Figure 11: The prompts for zero-shot testing.

F ADDITIONAL STUDY

Table 7: DeCLIP zero-shot performance of ImageNet top1 on different training datasets.

BACKBONE	DATASET	DATA SIZE	BATCH SIZE	ZERO-SHOT
RESNET50	CONCEPTUALCAPTIONS	3M	2,048	27.8
RESNET50	CONCEPTUAL12M	11M	4,096	41.0
RESNET50	YFCC	15M	4,096	41.9
RESNET50	DECLIP OPEN-SOURCE DATA	29M	6,144	49.3

Different Pre-training Datasets Data is critical for language-image pre-training task. As shown in Tab. 7, we evaluate our DeCLIP on different sources of datasets. Combining Tab.7 and Fig.1, we can see that when the amount of training data continues to scale up, the zero-shot recognition ability continues to improve as well. In addition, we can see that the open source data has high quality. The 29M open source data can achieve 49.3% zero-shot top1 accuracy on ImageNet through the DeCLIP training paradigm. Our open-source data is an affordable benchmark, which would be beneficial for explorations.

Our YFCC re-implementation Although we use the same number of image-text pairs as the CLIP YFCC-15M, our YFCC data is different from CLIP. We also reproduce the naive CLIP on our YFCC-15M data, which results in 35.9% zero-shot top1 accuracy on ImageNet-1K (see Fig. 8). It is relatively higher than the number in CLIP paper (31.1%). We conjecture the improvements might be caused by the different data cleaning strategies. However, our DeCLIP can achieve 41.9% zero-shot accuracy which is also 6.0% higher than our CLIP re-implementation.

Table 8: DeCLIP zero-shot performance of ImageNet top1 on YFCC datasets. Although we use the same amount of data, our YFCC is different with CLIP YFCC due to the different data cleaning strategies.

MODEL	BACKBONE	DATASET	DATA SIZE	BATCH SIZE	ZERO-SHOT
CLIP	RESNET50	YFCC	15M	—	31.3
CLIP (OUR REIMP.)	RESNET50	YFCC*	15M	4,096	35.9
DECLIP	**RESNET50**	**YFCC***	**15M**	**4,096**	**41.9(↑+6.0)**

Memory usage Because of the additional views, our DeCLIP is more memory-consuming. Thanks to the ICLR anonymous review comments: a fairer comparison might be doubling the batch size of CLIP. Flowing the ablation study in Fig. 7, we double the batch size and train CLIP-ResNet50 for 64 epochs. The final result is 22.3% which is still 4.9% lower than our DeCLIP model. We summarize the memory usage, training cost, and the final accuracy as below. All experiments are conducted on CC-3M with 16 V100 GPUs.

Table 9: Ablation on Memory usage.

MODEL	BATCH SIZE PER GPU	MEMORY (GB)	EPOCHS	COST (GPU HOURS)	ZERO-SHOT
CLIP-RESNET50	128	15.8	64	416	21.7
CLIP-RESNET50	256	24.0	64	399	22.3
DECLIP-RESNET50	128	22.7	32	304	27.2